

## Electronic Structure of $\text{Nd}_{1-x}\text{Sr}_x\text{FeO}_3$ Probed by Soft-X-Ray Spectroscopy

Tohru Higuchi,<sup>1\*</sup> Naoya Suzuki,<sup>1</sup> Makoto Minohara,<sup>2</sup> Masaki Kobayashi<sup>2</sup> and Hiroshi Kumigashira<sup>2</sup>

<sup>1</sup>Department of Applied Physics, Tokyo University of Science, Tokyo 125-8585, Japan

<sup>2</sup>Photon Factory, KEK, Tsukuba 305-0801, Japan

The electronic structure of  $\text{Nd}_{1-x}\text{Sr}_x\text{FeO}_3$  ( $x=0, 0.1$  and  $0.4$ ) has been studied by soft-X-ray spectroscopy. The  $\text{Nd}_{1-x}\text{Sr}_x\text{FeO}_3$  has the mixed valence states of  $\text{Fe}^{3+}$  and  $\text{Fe}^{2+}$ . The intensity of hole-induced state at the bottom of the conduction band increases with increasing Sr concentration. The valence band is mainly composed of the  $\text{O}2p$  state hybridized with the  $\text{Fe} 3d$  state. The resonant photoemission spectra of  $\text{Nd}_{0.9}\text{Sr}_{0.1}\text{FeO}_3$  exhibit the  $e_g$ -subband of  $\text{Fe} 3d$  state at near  $E_F$ , which is closely related to the electrical conductivity at room temperature.

### 1 Introduction

Sr-doped  $\text{NdFeO}_3$  ( $\text{Nd}_{1-x}\text{Sr}_x\text{FeO}_3$ ) with perovskite structure is expected as a  $p$ -type thermoelectric material due to its high chemical stability in air. The electrical conductivity for the oxygen gas partial pressure exhibits hole-ion mixed conduction, which needs for electrode of solid state oxide fuel cell (SOFC), at high temperature region [1]. The mixed conduction is useful for the performance of SOFC. However, details of structural and electrical properties have not been clarified far.

In this study, the authors have prepared the  $\text{Nd}_{1-x}\text{Sr}_x\text{FeO}_3$  bulk ceramics and probed their electronic structures by X-ray absorption spectroscopy (XAS) and high-resolution photoemission spectroscopy (PES). The  $\text{Nd}_{1-x}\text{Sr}_x\text{FeO}_3$  has hole and oxygen vacancies in the crystal lattice by Sr substitution. In this paper, the authors discuss about the valence state of Fe, oxygen vacancies and electronic structures of the valence band for  $\text{Nd}_{1-x}\text{Sr}_x\text{FeO}_3$  ( $x=0, 0.1, 0.2$ , and  $0.4$ ) in comparison with electrical conductivity.

### 2 Experiment

$\text{Nd}_{1-x}\text{Sr}_x\text{FeO}_3$  ( $x=0, 0.1, 0.2$ , and  $0.4$ ) bulk ceramics were prepared by the solid-state reaction method.  $\text{Nd}_2\text{O}_3$ ,  $\text{SrCO}_3$  and  $\text{Fe}_2\text{O}_3$  powders were mixed using a wet ball mill. The mixture was pressed into a disk shape at 14 kN and sintered for 24 h at  $1300^\circ\text{C}$ . The crystallization of the prepared target was confirmed using X-ray diffraction (XRD) using  $\text{CuK}\alpha$ .

The electronic structure was confirmed by photoemission spectroscopy (PES) and X-ray absorption spectroscopy (XAS), which was installed at the undulator beamline BL-2A in Photon Factory, KEK. The XAS spectra were measured by total-electron-yield mode. The kinetic energy of photoelectron for PES was measured using Gammadata-Scientia SES-2002. The energy resolutions of PES and XAS were 100 meV and 60 meV, respectively, at  $h\nu=700$  eV. The energy axis was calibrated by measuring Au film evaporated onto the manipulator in all measurements.

### 3 Results and Discussion

Table 1 shows peak positions of (110), (112) and (202) for Sr concentration estimated from XRD patterns. The (110) and (112) peaks shifts to higher diffraction angle

side and (202) peak shifts to lower diffraction angle side with increasing Sr concentration. This result indicates that the lattice constant of  $a$ -axis increases and those of  $b$ - and  $c$ -axes decrease with Sr concentration.

Table 1 Peak positions of (110), (112) and (202) for the XRD patterns

	(110)	(112)	(202)
$x=0$	$22.78^\circ$	$32.50^\circ$	$40.36^\circ$
$x=0.1$	$22.86^\circ$	$32.54^\circ$	$40.32^\circ$
$x=0.2$	$22.88^\circ$	$32.58^\circ$	$40.26^\circ$
$x=0.4$	$22.90^\circ$	$32.64^\circ$	$40.20^\circ$

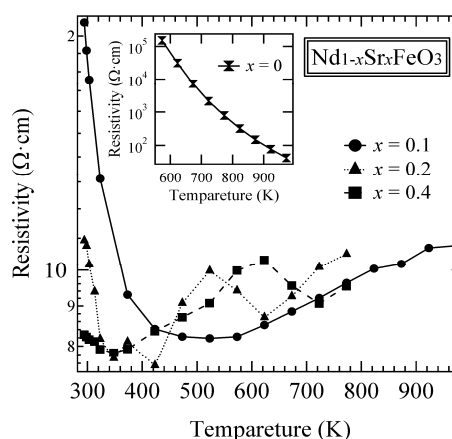


Fig.1 Temperature dependence of electrical resistivity of  $\text{Nd}_{1-x}\text{Sr}_x\text{FeO}_3$  ( $x=0, 0.1, 0.2$ , and  $0.4$ ).

Figure 1 shows the temperature dependence of electrical resistivity of  $\text{Nd}_{1-x}\text{Sr}_x\text{FeO}_3$ . The  $\text{NdFeO}_3$  exhibits insulator-like behavior. The resistivities of  $x=0.1$  and  $0.2$  decrease with decreasing temperature between 400 and  $1000^\circ\text{C}$ . However, those increase below  $400^\circ\text{C}$ . On the other hand, the resistivity of  $x=0.4$  decreases with decreasing temperature, which corresponds to the metallic behavior. The resistivity of  $\text{Nd}_{1-x}\text{Sr}_x\text{FeO}_3$  is lower than that of  $\text{La}_{1-x}\text{Sr}_x\text{FeO}_3$ .

Figure 2 shows the  $\text{Fe} 2p$  XAS spectra of  $\text{Nd}_{1-x}\text{Sr}_x\text{FeO}_3$ . Each spectrum consists of two parts derived from the spin-orbit split of  $L_3$  ( $2p_{3/2}$ ) and  $L_2$  ( $2p_{1/2}$ ) states. They are

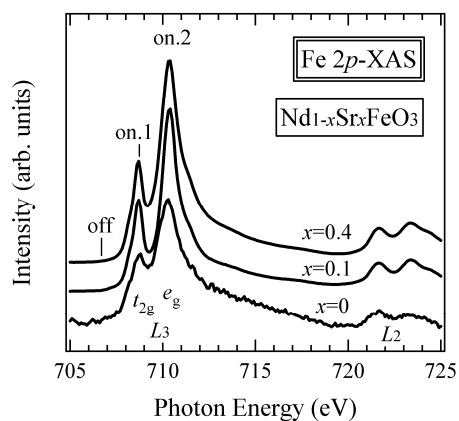


Fig. 2 O 1s XAS spectra of  $\text{Nd}_{1-x}\text{Sr}_x\text{FeO}_3$  ( $x=0, 0.1, 0.2,$  and  $0.4$ ).

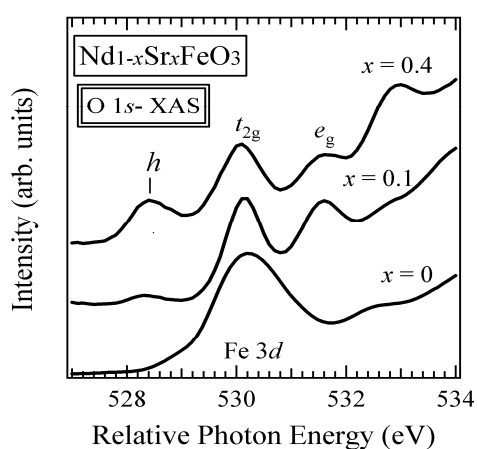


Fig. 3 Fe 2p XAS spectra of  $\text{Nd}_{1-x}\text{Sr}_x\text{FeO}_3$  ( $x=0, 0.1, 0.2,$  and  $0.4$ ).

further split into the  $t_{2g}$  and  $e_g$  states due to the octahedral ligand field. The crystal-field splitting ( $10Dq$ ) corresponding to the energy separation between  $t_{2g}$  and  $e_g$  states is 1.5 eV. The spectral shape and peak position are similar to those of  $\text{La}_{1-x}\text{Sr}_x\text{FeO}_3$ , which was calculated assuming a high-spin  $[t_{2g}]^3[e_g]^2$  ground state [2]. The intensity of  $t_{2g}$ -subband increases with Sr concentration, indicating that the doped Sr ions are doped as hole.

Figure 3 shows the O 1s-XAS spectra of  $\text{Nd}_{1-x}\text{Sr}_x\text{FeO}_3$ . The O 1s XAS of Fe oxide corresponds to the transition from O 1s core level to unoccupied O 2p state hybridized with Fe 3d state. The conduction band is mainly composed of Fe 3d state. Hole or oxygen vacancies induced state ( $h$ ) is observed at the bottom of the conduction band. The intensity of the structure increases with Sr concentration.

Figure 4 shows the resonant-PES spectra of  $\text{Nd}_{0.9}\text{Sr}_{0.1}\text{FeO}_3$  measured at various excitation energies. The off-resonance spectrum reflects the O 2p states without Fe 3d state. The intensity of on.1 spectrum corresponding to  $t_{2g}$ -resonance is enhanced in the valence band region, indicating the hybridization effect between

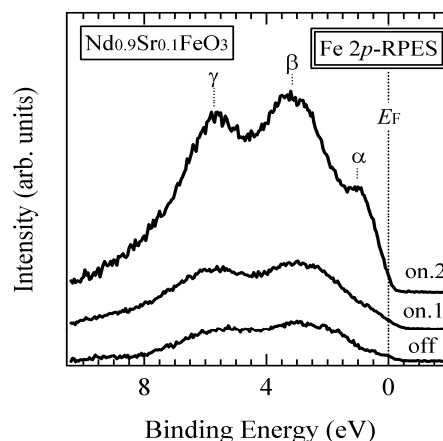


Fig. 4 Fe 2p resonant PES spectra of  $\text{Nd}_{0.9}\text{Sr}_{0.1}\text{FeO}_3$  measured at various excitation energies of Fig. 3.

O 2p state and Fe 3d ( $t_{2g}$ ) state. The on.2 spectrum corresponding to  $e_g$ -resonance exhibits strong resonance effect at peak  $\alpha$  at near the Fermi level ( $E_F$ ). This result indicates that the  $e_g$ -subband of Fe 3d state is closely related to the electrical conductivity of  $\text{Nd}_{0.9}\text{Sr}_{0.1}\text{FeO}_3$ .

#### 4 Summary

We have studied the electrical resistivities and electronic structures of  $\text{Nd}_{1-x}\text{Sr}_x\text{FeO}_3$ . The lattice constant of  $a$ -axis increases and those of  $b$ - and  $c$ -axes decrease with Sr concentration. The Fe has the mixed valence states of  $\text{Fe}^{2+}$  and  $\text{Fe}^{3+}$ . The hole-induced state with Sr doping is observed at the bottom of the conduction band. The valence band is mainly composed of  $t_{2g}$ - and  $e_g$ -subbands of Fe 3d states hybridized with O 2p states. The electrical conductivity of  $\text{Nd}_{0.9}\text{Sr}_{0.1}\text{FeO}_3$  is achieved by the  $e_g$ -subband at  $E_F$ .

#### References

- [1] K. Kobayashi, S. Yamaguchi, T. Higuchi, S. Shin, T. Tsukamoto and T. Tsunoda, *Electrochemistry* **72** (2004) 870.
- [2] H. Wadati, A. Chikamatsu, M. Takizawa, R. Hashimoto, H. Kumigashira, T. Yoshida, T. Mizokawa, A. Fujimori, M. Oshima, M. Lippmaa, M. Kawasaki, and H. Koinuma, *Phys. Rev. B* **74** (2006) 115114.

#### Research Achievements

1. T. Higuchi, T. Owaku, Y. Iida, E. Sakai, M. Kobayashi and H. Kumigashira; *Solid State Ionics* **270** (2014) 1.
2. S. Yamaguchi, Y. Tasaki, M. Kobayashi, K. Horiba, H. Kumigashira, and T. Higuchi; *Jpn. J. Appl. Phys.* **54** (2015) 06FJ04.
3. Y. Shimazu, T. Okumura, T. Tsuchiya, A. Shimada, K. Tanabe, M. Kobayashi, K. Horiba, H. Kumigashira and T. Higuchi; *J. Phys. Soc. Jpn.* **84** (2015) 064701.

\* higuchi@rs.kagu.tus.ac.jp